van Bergeijk, Vera; Warmink, Jord; Frankena, Marc; Hulscher, Suzanne

Modelling Dike Cover Erosion by Overtopping Waves: The Effects of Transitions

Coastal Structures 2019 - Nils Goseberg, Torsten Schlurmann (eds) - © 2019 Bundesanstalt für Wasserbau
ISBN 978-3-939230-64-9 (Online) - DOI: 10.18451/978-3-939230-64-9_110

Modelling Dike Cover Erosion by Overtopping Waves: The Effects of Transitions

V. M. van Bergeijk, J. J. Warmink, M. Frankena & S. J. M. H. Hulscher
University of Twente, Enschede, The Netherlands

Abstract: A new wave overtopping-erosion model is developed to find the weakest point across the dike. This analytical model calculates the maximum flow velocity and the erosion depth along a dike profile for a series of overtopping waves. The effect of transitions on the flow and the erosion depth downstream are incorporated in this model, since the model is applied to entire dike profile. Transitions in geometry and bed roughness result in local deceleration and acceleration of the flow affecting the erosion depth significantly. A storm is simulated by generating a distribution of overtopping wave volumes, which are used to determine the hydraulic boundary conditions. The model is applied to the Lake Ijssel side of the Afsluitdijk in the Netherlands. The weakest point along this profile was located next to a berm with both transitions in slope angle and bed roughness. The model results look promising, however, a short sensitivity analysis showed that formulations for the erosion parameters need to be improved to make the model general applicable.

Keywords: Wave overtopping, Analytical model, Turbulence, Cover erosion, Transitions

1 Introduction

During storms, waves exert high forces on flood defences. Often, the watersides of flood defences are covered in revetments such as stones and asphalt to withstand these wave forces. However, the crest and the landward side of flood defences such as dikes and embankments are often covered in grass. The grass cover makes these flood defences vulnerable for overtopping waves that flow over the crest and accelerate on the landward slope. The erosion of a grass cover by overtopping waves is a complex process. The shape and the speed of the overtopping wave change across the profile resulting in variations of the load (Schüttrumpf and Oumeraci, 2005; Van Bergeijk et al., 2019). Also, changes in cover type and geometry across the flood defence affect the hydraulic load and the cover strength significantly (Bomers et al., 2018; Warmink et al., 2018). These processes result in variations in the amount of cover erosion across the flood protective structure. Once the cover is eroded at one location, the core material of the flood defence starts to erode resulting in weakening of the structure and, in the end, in a breach (Oumeraci, 2005).

Several methods have been developed to model the cover erosion by overtopping waves. Studies by Whitehead (1976) and Hewlett et al. (1987) resulted in velocity-duration curves to determine the maximum allowed velocity for a certain duration of overflow for different grass qualities. Dean (2010) used these curves to determine the best erosional index for grass cover erosion by combined overflow and wave overtopping: flow velocity, shear stress or work. This method accounts for the time-varying characteristics of wave overtopping flow and can be applied to determine the erosional effects of multiple storms. The cumulative overload method was developed by Van der Meer (2010) using data of overtopping tests on grass-covered dikes in the Netherlands. The cumulative overload method is based on the shear stress formulation of Dean (2010) and adapted for solely wave overtopping.

The erosion models mentioned so far have two shortcomings: (a) they result in one value for the maximum allowed flow velocity or failure along the entire profile and (b) they are only applicable to a specific location along the profile. The configuration of a flood defence consists often of multiple cover types and several geometrical transitions, such as a berm. The previous mentioned models need to be applied to every part of the profile separately. Transitions on the crest and the slope affect the flow downstream, thus it is important to consider the entire dike profile in the computation. Moreover, if the output of interest is to find the weakest point along the profile, a model for erosion along the profile is required. For these reasons, a model for cover erosion by overtopping waves that can be applied to the entire profile and takes the effect of transitions on the downstream flow and erosion into account is beneficial.

The erosion model developed by Hoffmans (2012) is able to calculate the erosion depth along the profile once the flow velocity along the profile is known. This erosion model was coupled to a CFD model to study the erosional effect of a road on the dike crest (Aguilar-López et al., 2018; Bomers et al., 2018). The coupled hydrodynamic-erosion model was able to reasonably simulate the location and the amount of erosion compared to experimental data (Bomers et al., 2018). However, the model domain was limited to the dike crest and a small part of the slope due to high computational costs of the CFD models. Also, the models did not consider all wave volumes simulated during the wave overtopping tests. Aguilar-López et al. (2018) used emulators to test different storm scenarios, while Bomers et al. (2018) discretized the distribution of overtopping waves and only modelled five representative wave volumes to simulate the erosion depth after a storm.

The recently developed analytical model for overtopping flow velocities of Van Bergeijk et al. (2019) calculates the flow velocity along the dike profile for several dike geometries and cover types. These analytical formulas are computationally fast; thus, enabling to model the cover erosion for several storm scenarios and a series of overtopping wave volumes. Although the modelled flow velocities are depth-averaged, the effect of turbulence on the dike cover erosion is still included by means of a turbulence parameter in the erosion model of Hoffmans (2012).

This paper describes a new coupled wave overtopping-erosion model to determine the cover erosion along the dike profile during a storm. This model takes the effect of transitions on the flow and cover erosion downstream into account by directly calculating the erosion depth along the entire dike profile. The model set-up and the necessary input parameters are described in Section 2. The model is applied to the Lake Ijssel side of the Afsluitdijk, the Netherlands (Section 3). This dike profile contains several geometrical transitions as well as transitions in cover type. The model is used to find the weakest point along the profile and the results are described in Section 4. A short sensitivity analysis to the erosion model is presented in the discussion (Section 5) and the conclusions are stated in Section 6.

2 The analytical wave overtopping-erosion model

2.1 Model set-up

The analytical model determines the wave overtopping flow velocity and the cover erosion along the dike profile. The analytical formulas for the maximum overtopping flow velocity of Van Bergeijk et al. (2019) are coupled to an erosion formula based on the erosion model of Hoffmans (2012). The required hydrodynamic boundary conditions are the flow velocity at the start of the crest U_0 and the momentary discharge Q of the overtopping wave (Van Bergeijk et al., 2019). Besides the flow velocity along the profile, the erosion model requires several input parameters including the critical flow velocity U_c and the turbulence intensity parameter r_0.

The analytical model calculates the erosion depth after one storm along the crest and the landward side of the dike. Overtopping wave volumes during the storm are sampled from a probability distribution based on the storm duration and the number of overtopping waves (Section 2.3). For each overtopping wave i, the flow velocity at the start of the crest $U_{0,i}$ and the discharge Q,i are determined using the overtopping volume. Next, the model calculates the flow velocity and the erosion depth along the profile for each overtopping wave (Fig. 1b). The coupled model simulates the erosion depth for all overtopping waves, and, in the end, the erosion depths of all waves are summed to obtain the total erosion depth after the storm.

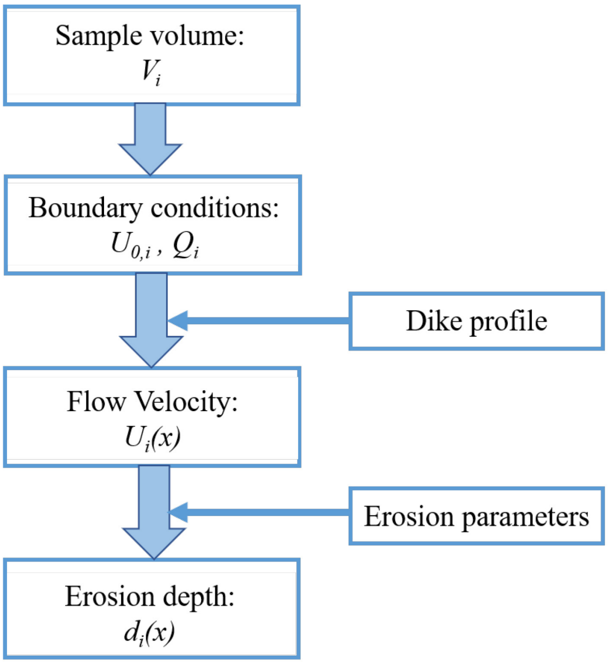

Fig. 1. Schematization of the coupled wave overtopping-erosion model. An overtopping volume V_i is sampled which is used to determine the required boundary conditions for each overtopping wave i: the flow velocity $U_{0,i}$ and the discharge Q_i at the start of the crest. Using the dike profile, the flow velocity $U_i(x)$ as a function of the cross-dike coordinate x is calculated. Next, the erosion depth along the dike $d_i(x)$ of one individual wave is calculated using the flow velocity and the erosion parameters.

2.2 *The analytical formulas of the wave overtopping-erosion model*

The erosion model of Hoffmans (2012) is adapted to account for variations in the hydraulic load and cover strength along the dike profile. The erosion depth d of one overtopping wave is calculated as

$$d(x) = \left(\omega(x)^2 U^2(x) - U_c^2(x)\right) T_0 C_E \qquad \text{for } \omega(x)U(x) \geq U_c(x), \tag{1}$$

with the cross-dike coordinate x, the flow velocity U, the critical flow velocity U_c, the overtopping period T_0 and the strength parameter C_E. The turbulence parameter ω depends on the turbulence intensity r_0 as

$$\omega(x) = 1.5 + 5r_0(x). \tag{2}$$

According to this model, erosion occurs when the load (ωU) exceeds the cover strength (U_c). The erosion rate is described by the strength parameter C_E and the erosion time is described by T_0. Transitions influence the amount of turbulence, the flow velocity and the cover strength, so these parameters depend on the cross-dike coordinate.

The flow velocity along the cross-dike profile is calculated using the formulas derived by Van Bergeijk et al. (2019). These formulas describe the flow velocity along a horizontal part of the dike profile $U_{horizontal}$, such as the crest or a berm, and the flow velocity along a slope U_{slope}.

$$U_{horizontal}(x) = \left(\frac{fx}{2Q} + \frac{1}{U_{horizontal}(x=0)}\right)^{-1}, \tag{3}$$

$$U_{slope}(x) = \frac{\alpha}{\beta} + \mu\, exp(-3\alpha\beta^2\, x/cos\varphi)\,, \tag{4}$$

with the bottom friction coefficient f, the discharge Q and the slope angle φ. The parameters μ, α and β are given by

$$\mu = U_{slope,0} - \frac{\alpha}{\beta},\ \ \alpha = \sqrt[3]{gsin\varphi} \ \text{ and } \ \beta = \sqrt[2]{f/2\,Q} \tag{5}$$

with the flow velocity at the start of the slope $U_{slope,0}$ and the gravitational acceleration g.

The effect of transitions on the flow velocity is included in these formulas. Transitions in cover roughness are modelled by adapting the bottom friction parameter f and geometrical transitions are modelled using the slope angle φ. Multiple parts of the dike profile are coupled by using the overtopping flow velocity at the end of one part as input value for the flow velocity of the next profile part.

2.3 Boundary conditions and input parameters

The overtopping volume of the individual waves during the storm are determined using the exceedance distribution in the EurOtop Manual (2007). The exceedance distribution describes the probability P_V that an overtopping volume V_i is smaller than the volume V

$$P_V(V_i \leq V) = 1 - exp[-(V/a)^{0.75}] , \tag{6}$$

where

$$a = 0.84\, q_m\, t_{storm}/N_{ow}, \tag{7}$$

and the mean overtopping discharge q_m, the duration of the storm t_{storm} and the number of overtopping waves N_{ow}. The individual overtopping volumes are used to determine the boundary conditions for the analytical flow model (Fig. 1).

The boundary conditions U_0 and Q depend on the overtopping volume and are determined using the empirical formulas of Van der Meer et al. (2010)

$$U_0 = 4.5\, V^{0.3}, \tag{8}$$

$$h_0 = 0.133\, V^{0.5}, \tag{9}$$

$$Q = U_0\, h_0. \tag{10}$$

The overtopping period T_0 is calculated using the empirical relation by Hughes (2012),

$$T_0 = 3.9\, V^{0.46}. \tag{11}$$

Next to the hydrodynamic boundary conditions, a dike profile is required as input for the model. Each part of the dike is described by a slope angle φ and a bottom friction coefficient f for the roughness of the cover. For the erosion model, the strength of the dike cover is described by the critical flow velocity U_c which depends on the cover type. The strength parameter C_E was set to $2 \cdot 10^{-6}$ s/m corresponding to an average grass quality (Hoffmans, 2012).

3 Case study: Afsluitdijk

The coupled erosion model is applied to the Afsluitdijk in the Netherlands to find the weakest point along the profile (Fig. 2). The profile of the Afsluitdijk includes multiple berms and transitions between grass and asphalt (Fig. 2 and 3e). A biking path is located on the upper most berm around a cross-dike distance of 12 m and two roads are located on the lower berm at x = 17 m. The slope steepness varies between 1:2 and 1:4.5 and the bottom friction coefficient f is 0.01 and 0.02 for grass and asphalt, respectively. The critical flow velocity U_c was set to a constant value of 8 m/s (Van Hoven and Van der Meer, 2014). A storm is simulated using a storm duration t_{storm} of 6 h with 525 overtopping waves corresponding to a mean overtopping discharge q_m = 5 l/s/m. The sea wave regime consists of a significant wave height H_s = 2.0 m and the peak period T_p = 5.7 s.

The modelled overtopping flow velocities are depth-averaged; thus, the effect of turbulence is included in the erosion model through the turbulence intensity r_0. Transitions in roughness and geometry affect the turbulence and by that the amount of dike cover erosion. Three formulations for the turbulence intensity are tested to determine the sensitivity of the erosion model to the turbulence intensity.

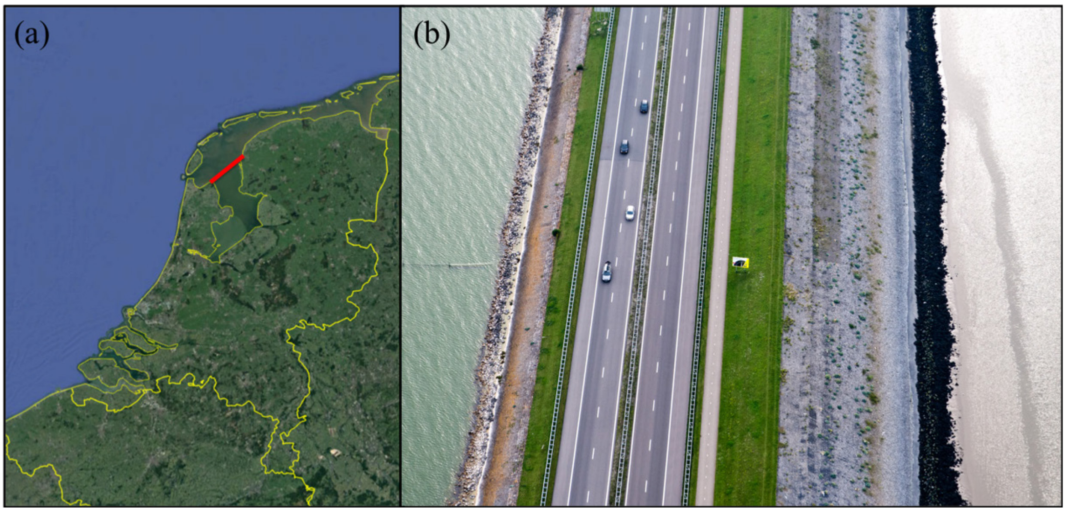

Fig. 2. (a) The location of the Afsluitdijk in the Netherlands. (b) Photo of the cross-dike profile of the Afsluitdijk with the Lake Ijssel on the left and the Wadden Sea on the right (Retrieved from https://beeldbank.rws.nl/).

3.1 Formulation A: Constant

The first formulation is a constant turbulence intensity r_0 along the cross-dike profile, assuming that transitions do not influence the amount of turbulence. The turbulence intensity is set to 0.1 (Red, Fig. 3c) according to measurements on the crest during overtopping experiments (Bomers et al., 2018).

3.2 Formulation B: Hoffmans (2012)

Hoffmans (2012) reported two formulas for the turbulence intensity. The turbulence intensity on horizontal parts of the profile solely depends on the cover roughness through the bottom friction coefficient *f*

$$r_0 = 0.85\sqrt{f}\ . \tag{12}$$

The turbulence intensity on the slope depends on the slope angle φ and the maximum flow velocity on the slope U_{max}

$$r_0 = \sqrt{\frac{gQsin\varphi}{U_{max}^3}}. \tag{13}$$

The cover roughness and slope angle vary along the profile resulting in a varying turbulence intensity r_0 along the profile (Yellow dashed, Fig. 2c). The turbulence intensity is smaller on the slope compared to the horizontal parts of the profile. Also, the turbulence intensity is smaller for grass than asphalt, because the friction coefficient of grass is smaller.

3.3 Formulation C: Turbulence input from mixing

Turbulent mixing in the boundary layer depends on the cover roughness and the slope angle. The mixing term is related to the double gradient of the flow velocity, which increases significantly at transitions (Fig. 3ab). At transitions, additional turbulence is created by local acceleration and deceleration of the flow. This formulation increases the turbulence intensity with 0.1 at locations where mixing is important:

$$|\partial^2 U/\partial x^2| > 0\ . \tag{14}$$

The extra turbulence input decreases to the background turbulence intensity of 0.1 over a length of 1 m (Purple dotted, Fig. 3c). The background value equals the constant turbulence intensity of formulation A.

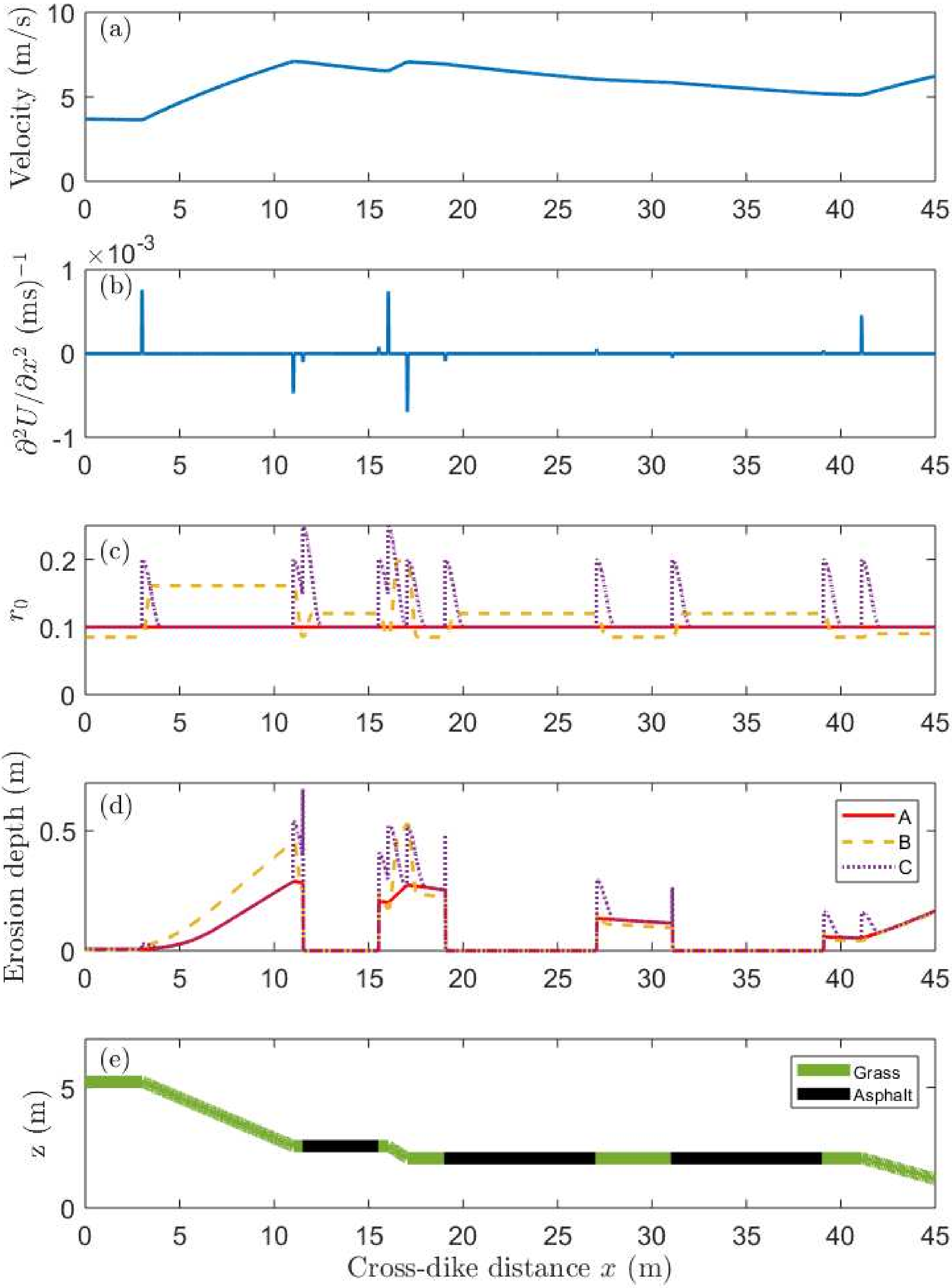

Fig. 3. (a) The 2% exceedance flow velocity as function of the cross-dike coordinate x. (b) The mixing term related to the double gradient of the flow velocity U increases at transitions. (c) The turbulence intensity r_0 as function of the cross-dike distance x for the three formulations A, B and C. (d) The erosion depth after a storm for the three formulations of the turbulence intensity. (e) The dike profile of the Lake Ijssel side of the Afsluitdijk.

4 Results

The modelled 2% exceedance flow velocity during the simulated storm is smaller than the critical flow velocity of 8 m/s (Fig. 3a). However, the flow velocity is multiplied by a turbulence parameter to obtain the load in the erosion model, so significant erosion occurs during the storm. The three turbulence formulations result in a maximum erosion depth of 0.29 m, 0.53 m and 0.67 m for formulation A, B and C, respectively (Fig. 3d). It is interesting to note that the location of maximum erosion x_{max} is different for formulation B (x_{max} = 17 m) compared to formulation A (x_{max} = 11 m) and C (x_{max} = 11.5 m). According to formulation B, the weakest point of the Afsluitdijk is downstream of the biking path while the other two formulations indicate the grass cover upstream of the biking path as weakest point. Both results agree with a study on the erosion resistance of the Afsluitdijk using the cumulative overload method by Van Hoven and Van der Meer (2014). They identified the grass cover upstream and downstream of the biking path as most erosion prone because of an increasing load due to changes in cover roughness.

5 Discussion

5.1 Relations between the erosional parameters

The threshold of erosion is determined by the critical flow velocity and the turbulence intensity. These parameters – together with the flow velocity along the dike profile - determine the locations where erosion occurs. When the critical flow velocity and the turbulence intensity are determined from calibration, multiple combinations can lead to the same result. For example, an increase in the turbulence intensity can be balanced by a decrease in the critical flow velocity to obtain similar results for the erosion depth.

The relation between the critical flow velocity and turbulence intensity is shown in a model study of an overtopping experiment on a grass covered dike with an asphalt road on the dike crest at Millingen a/d Rijn (Van Hoven et al., 2013; Bomers et al., 2018). Overtopping waves with an average overtopping discharge of 50 l/s/m were released to simulate a 6-hour storm with a significant wave height of 1 m and a peak period of 4 s. At the end of the experiment, the erosion depth along the dike profile was measured. The same 6-hour storm is modelled using the same parameters as the experiment with 4583 overtopping waves. The profile is split in four parts: (1) the grass-covered crest upstream of the road, (2) the road, (3) the grass-covered crest downstream of the road, and (4) the grass-covered slope (Fig 4a). The value of the critical flow velocity is calibrated by adapting the U_c value until the modelled erosion profile matches the observed erosion profile, while keeping the turbulence intensity constant along the profile. The calibration was done separately for the four parts of the profile and for two values of the turbulence intensity: $r_0 = 0$ and $r_0 = 0.1$.

The calibrated critical flow velocity increases between 30% and 300% to balance the increase of the turbulence intensity r_0 by 0.1 (Tab. 1, Fig. 4). The calibrated critical flow velocity is small on the downstream side of the asphalt road and approximately twice as large on the slope compared to the crest. The large differences in the calibrated critical flow velocity indicate that either the turbulence intensity varies along the dike profile - as adapted in the model of the Afsluitdijk - or the critical flow velocity varies along the profile as was done in this case.

Tab. 1. Calibrated values of the critical flow velocity U_c for grass in m/s for the Millingen a/d Rijn for a constant turbulence intensity r_0 of 0 and 0.1

Location	$r_0 = 0$	$r_0 = 0.1$
(1) Grass-covered crest upstream of the road	6	9
(2) Asphalt road	-	-
(3) Grass-covered crest downstream road	1	4
(4) Grass-covered slope	13	17

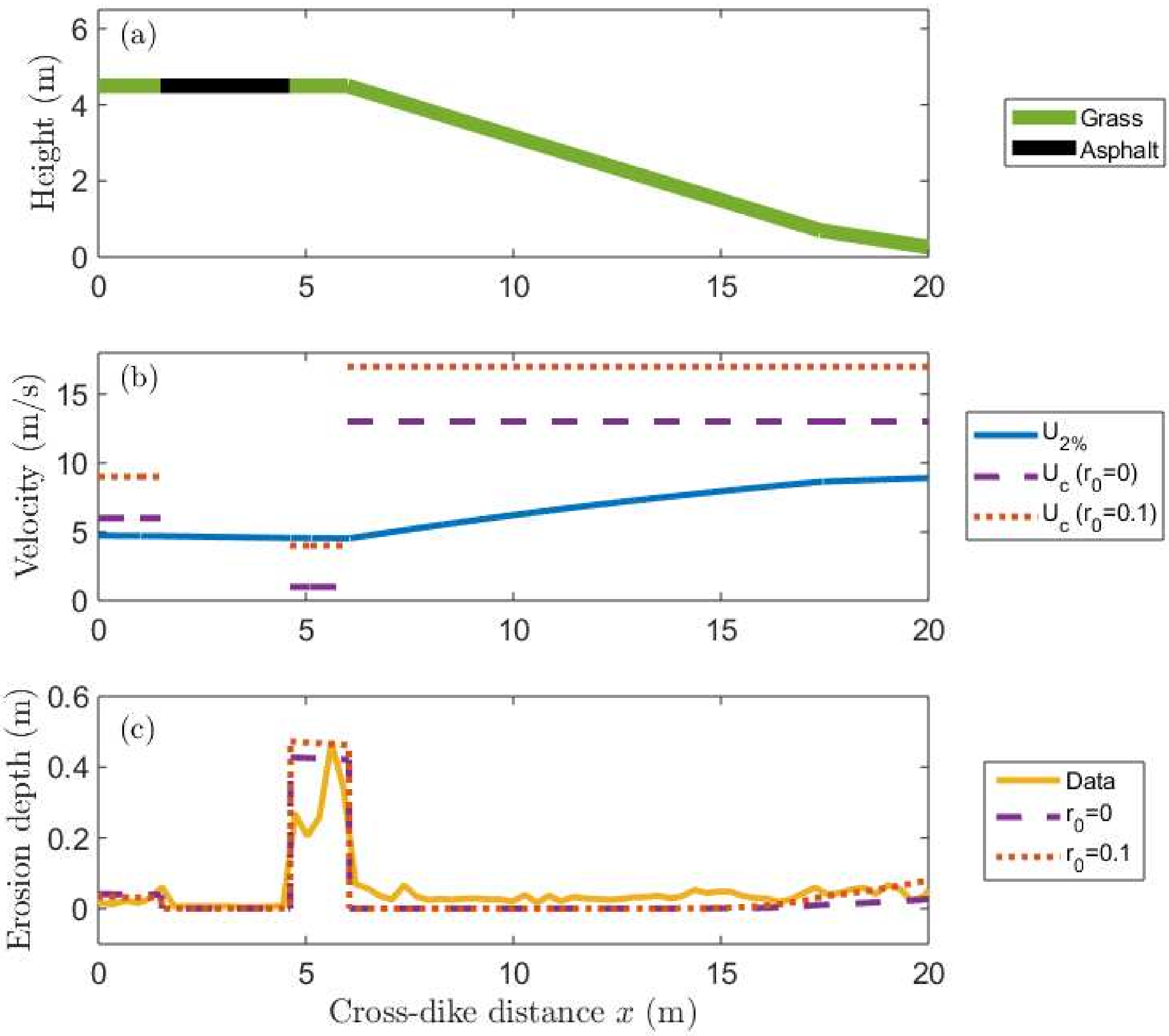

Fig. 4. (a) The configuration of the grass-covered dike at Millingen a/d Rijn with an asphalt road on top of the crest. (b) The modelled 2% exceedance flow velocity $U_{2\%}$ of the storm and the calibrated value of critical flow velocity U_c for both value of the turbulence intensity r_0. (c) The modelled and measured erosion depth for a storm with an average overtopping discharge of 50 l/s/m/.

The strength parameter C_E does not affect the location, but the amount of erosion. This parameter is assumed constant along the profile in the study; however, the strength parameters depends on the critical flow velocity (Hoffmans, 2012). Thus, the wave overtopping-erosion model contains three parameters that affect the erosion depth and the location of erosion. For that reason, multiple combinations of these parameters are possible in case of calibration. The model needs to be applied to more cases to validate formulations for the three parameters, for example the formulations proposed by Hoffmans (2012) and Valk (2009). Further research into methods to determine the erosion parameters independently is recommended.

5.2 Application of the model

We introduced a new wave overtopping-erosion model that is able to find the weak spots along a dike profile. The model results look promising, however, there are still some challenges to make this model general applicable.

- *Challenge 1: improving the estimates of the strength parameter C_E for more grass types and other soil types.* The erosion rate is determined by the strength parameter C_E, thus, the strength parameter affects the erosion depth significantly. It is known that the strength parameter depends on the soil type am changes with depth. However, accurate estimates of the strength parameter are currently not available.

- *Challenge 2: improving the description of turbulence as driving factor of erosion depth.* The calibrated values for the critical flow velocity are higher compared to the calibrated values in the cumulative overload model: 17 m/s (Tab. 1) compared to 7 m/s (Van Hoven et al., 2013) on the slope at Millingen for a turbulence intensity r_0 of 0.1. This difference can be caused by an overestimation of the strength parameter C_E, that was assumed constant during this study. Also, the formulation of the hydraulic load differs between both models. The hydraulic load in the wave overtopping-erosion model is defined as the product between the flow velocity and the turbulence parameter, while in the cumulative overload method the additional load by turbulence is only included at transitions. The turbulence parameter in the wave overtopping-erosion model increases the load significantly, resulting in a higher value of the critical flow velocity to obtain the same erosion depth. A small sensitivity analysis was performed on both parameters and new formulations for the turbulence intensity and critical flow velocity are currently developed.
- *Challenge 3: including morphological feedback.* The total erosion depth of a storm is calculated by summing over the erosion depths of the individual overtopping waves; thus, morphological feedback is not included in the model. In reality, the cover strength of the dike cover changes with depth (Valk, 2009) and the height difference resulting from erosion create additional turbulence (Bomers et al, 2018). Morphological feedback is not possible using the analytical formulas of Van Bergeijk et al. (2019) since the dike geometry is modelled using a slope angle, so height differences cannot be incorporated. A CFD model is required for morphological feedback to include the effect of height differences on turbulence and the erosion depth.

These challenges also hold for other erosion models. Firstly, the relation between failure and the erosion rate is empirically determined for most erosion models with only little data available. The erosion model of Dean et al. (2010) solely used the velocity duration curves of Hewlett et al. (1987) and the failure definition in the cumulative overload method is based on one experiment (Van der Meer et al., 2014). Secondly, a load factor for turbulence is implemented in the cumulative load model to account for the effect of turbulence. Lastly, morphological feedback is not included in existing models, except in the study of Bomers et al. (2018) where the profile was updated every hour. For these reasons, solutions for these challenges will not only improve our new wave overtopping-erosion model but these solutions will also improve existing erosion models.

6 Conclusions

We developed a new wave overtopping-erosion model by coupling the formulas for the overtopping flow velocity of Van Bergeijk et al. (2019) to the erosion model of Hoffmans (2012). The model is able to calculate the erosion depth along the profile for a storm to find the weakest point along the dike profile. The model is computationally fast and can be used to calculate the erosion depth for several storm scenarios and multiple grass qualities. The advantage of this model is that the erosion depth along the entire dike profile is calculated. In this way, the model accounts for the effects of transitions on the downstream flow and erosion.

The model was applied to the Afsluitdijk where three formulations for the turbulence intensity were tested. The results showed that the turbulence intensity formulations affect both the location and the amount of erosion. The weakest point of the Afsluitdijk is the biking path, where the largest erosion depths were modelled. These model results compare well with the findings of Van Hoven and Van der Meer (2014).

A small sensitivity analysis on the erosion parameters was performed. From this analysis, we conclude that the turbulence intensity has a large influence on the erosion depth and that the threshold for erosion – modelled using the critical flow velocity – is higher for our wave overtopping-erosion model compared to other existing models. Improving the formulations for the erosion parameters is recommended to make the model general applicable.

Acknowledgements

This work is part of the research programme All-Risk, with project number P15-21, which is (partly) financed by the Netherlands Organisation for Scientific Research (NWO). We want to thank Paul van Steeg and Andre van Hoven from Deltares for their insights and useful suggestions on the modelling of transitions.

References

Aguilar-López, J.P., Warmink, J.J., Bomers, A., Schielen, R.M.J., Hulscher, S.J.M.H., 2018. Failure of grass covered flood defences with roads on top due to wave over- topping: a probabilistic assessment method. J. Mar. Sci. Eng. 6 (3), 74. https://doi.org/10.3390/jmse6030074.

Bomers, A., Aguilar-López, J.P., Warmink, J.J., Hulscher, S.J.M.H., 2018. Modelling effects of an asphalt road at a dike crest on dike cover erosion onset during wave overtopping. Nat. Hazards 93 (1), 1–30. https://doi.org/10.1007/s11069-018-3287-y.

ComCoast, 2007. Design, construction, calibration and the use of the of the wave overtopping simulator.

Dean, R. G., Rosati, J. D., Walton, T. L., and Edge, B. L., 2010. Erosional equivalences of levees: Steady and intermittent wave overtopping. Ocean Engineering, 37(1):104–113. https://doi.org/10.1016/j.oceaneng.2009.07.016

EurOtop Manual, 2007. Wave Overtopping of Sea Defences and Related Structures–Assessment Manual. UK: NWH Allsop, T. Pullen, T. Bruce. NL: JW van der Meer. DE: H. Schüttrumpf, A. Kortenhaus. www.overtopping-manual.com.

Hewlett, H. W. M., Boorman, L. A., & Bramley, L. A., 1987. Design of reinforced grass waterways. Construction Industry Research and Information Association.

Hoffmans, G. J., 2012. The influence of turbulence on soil erosion. Eburon Uitgeverij BV.

Hughes, S. A., Thornton, C. I., Van der Meer, J. W., & Scholl, B. N., 2012. Improvements in describing wave overtopping processes. Coastal Engineering Proceedings, 1(33), 35. https://doi.org/10.9753/icce.v33.waves.35.

Oumeraci, H., D'Eliso, C., and Kortenhaus, A., 2005. Breaching of coastal dikes: state of the art. Braunschweig, LWI Report number: 910.

Schüttrumpf, H. and Oumeraci, H., 2005. Layer thicknesses and velocities of wave overtopping flow at seadikes. Coastal Engineering, 52(6):473–495. https://doi.org/10.1016/j.coastaleng.2005.02.002

Valk, A., 2009. Wave overtopping impact of water jets on grassed inner slope transitions. TU Delft. Retrieved from http://resolver.tudelft.nl/uuid:5ca03ac7-0296-4ccd-b7b0-e9485cfc934f

Van Bergeijk, V. M., Warmink, J. J., van Gent, M. R. A, & Hulscher, S. J. M. H., 2019. An analytical model of wave overtopping flow velocities on dike crests and landward slopes. Coastal Engineering, 149, 28-38. https://doi.org/10.1016/j.coastaleng.2019.03.001

Van Hoven, A., Verheij, H., Hoffmans, G., & Van der Meer, J. W., 2013. Evaluation and model development: grass erosion test at the Rhine dike. Deltares Report, 1207811-002.

Van Hoven, A., Van der Meer, J., 2014. Analyse erosiebestendigheid Afsluitdijk. Deltares Report, 1207410-000-HYE-0007

Van der Meer, J. W., Hardeman, B., Steendam, G. J., Schüttrumpf, H., and Verheij, H., 2010. Flow depths and velocities at crest and landward slope of a dike, in theory and with the wave overtopping simulator, in: Coastal Engineering Proceedings. 1(32):10. https://doi.org/10.9753/icce.v32.structures.10

Van der Meer, J. W., Hoffmans, G., & Van der Hoven, A., 2014. Analyses grass erosion in wave run-up and wave overtopping conditions. Deltares report, 1209437-005-HYE-0003

Warmink, J. J., Van Bergeijk, V. M., Chen, W., Van Gent, M. R. A. & Hulscher, S. J. M. H., (2018). Modelling wave overtopping for grass covers and transitions in Dike Revetments, in Coastal Engineering Proceedings. 1(36): 53. https://doi.org/10.9753/icce.v36.papers.53

Whitehead, E., 1976. A guide to the use of grass in hydraulic engineering practice. HR Wallingford report 71.